

Circular RNA circ_0000034 upregulates STX17 level to promote human retinoblastoma development *via* inhibiting miR-361-3p

H. LIU, H.-F. YUAN, D. XU, K.-J. CHEN, N. TAN, Q.-J. ZHENG

Department of Ophthalmology, Daping Hospital, Army Medical Center of PLA, Chongqing, China

Abstract. – **OBJECTIVE:** Retinoblastoma (RB) is a common intraocular tumor of infancy and childhood. Circular RNAs (circRNAs) are related to the development of RB. The purpose of this research was to reveal the functional mechanism of circRNA circ_0000034 in RB.

MATERIALS AND METHODS: Quantitative Real-Time Polymerase Chain Reaction (qRT-PCR) and Western blot were applied to determine the levels of genes. MTT assay and flow cytometry were employed to assess cell proliferation and apoptosis rate, respectively. Furthermore, cell migratory and invasive abilities were measured using the transwell assay. Mouse xenograft was conducted to analyze the effect of circ_0000034 on tumor growth *in vivo*. Besides, the interaction between miR-361-3p and circ_0000034 or syntaxin 17 (STX17) was predicted by starBase, and then, confirmed by the Dual-Luciferase reporter assay and RNA immunoprecipitation (RIP) assay.

RESULTS: The levels of circ_0000034 and STX17 were increased and miR-361-3p level was decreased in RB tissues and cells. Circ_0000034 knockdown suppressed cell proliferation, migration, invasion, autophagy, and tumor growth, and induced apoptosis in RB. Circ_0000034 targeted miR-361-3p and miR-361-3p bound to STX17. Circ_0000034 overexpression and miR-361-3p knockdown reversed the effect of miR-361-3p upregulation and STX17 depletion on the growth of RB cells, respectively. Besides, circ_0000034 elevated STX17 level by repressing miR-361-3p expression.

CONCLUSIONS: We demonstrated that circ_0000034 knockdown suppressed the development of RB by the modulation of miR-361-3p/STX17 axis. Our findings provided a theoretical basis for the treatment of RB.

Key Words:

Circ_0000034, MiR-361-3p, STX17, Cell growth, Retinoblastoma.

Introduction

Retinoblastoma (RB), a normal intraocular tumor occurring in the retina, is diagnosed in

infants and children¹. According to the statistics, there are approximately 5,000 new cases of RB every year around the world². Nowadays, the combination of chemotherapy and immunotherapy is the major method for the therapy of RB, but this method is harmful to the RB cells³. Therefore, the studies of RB development mechanism are essential for the therapy of RB.

Circular RNAs (circRNAs), with long sequences, are a novel group of non-coding RNAs that contain closed loop and exist in a variety of tissues and cells in mammals^{4,5}. They were significantly involved in cancer cell progression, such as proliferation⁶, mobility⁷, apoptosis⁸, and autophagy⁹. Circ_0000034, identified as circRNA, was highly expressed in RB tissues compared with that in normal retinal tissues¹⁰, meaning that circ_0000034 might exert a function in the development of RB. However, the role and functional mechanism of circ_0000034 still need further investigations in RB cells.

MicroRNAs (miRNAs) mediate the levels of target genes via suppressing the translation or inducing degradation of messenger RNA (mRNA)^{11,12}. MiRNAs regulated the development of many human cancers, including bovine granulosa¹³, hepatocellular carcinoma¹⁴, renal carcinoma¹⁵, and RB¹⁶. Zhao et al¹⁷ demonstrated that miR-361-3p was lowly expressed in RB tissues and repressed the proliferation of RB cells. These results indicated that miR-361-3p played an important role in the development of RB. However, the detailed mechanism of miR-361-3p regulation in RB cells was less reported.

Syntaxin 17 (STX17) is an ER-resident syntaxin protein that is related to cell autophagy¹⁸. The evidence suggested that STX17 bound to syntaxosome-associated protein 29 (SNAP29) and vesicle-associated membrane protein 8 (VAMP8) to promote autophagosome-lysosome fusion by targeting the membrane of autophagosome^{18,19}. Furthermore, STX17 played a pivotal role in hu-

man cancers. Huang et al²⁰ suggested that STX17, regulated by long non-coding RNA MALAT1 (lncRNA MALAT1)/miR-124 axis, affected autophagy of RB cells. However, whether STX17 modulating other RB cell progression is unclear.

In this study, we detected the levels of circ_0000034, miR-361-3p, and STX17 in RB tissues and cells as well as analyzed the function of circ_0000034 in RB cell progression and tumor growth. Furthermore, circ_0000034 acted as an oncogene to promote RB cell growth was first reported and a new mechanism that circ_0000034 exerted function through regulating miR-361-3p/STX17 axis in RB cells was confirmed.

Materials and Methods

Tissues and Cell Culture

32 RB tissues and 6 normal tissues were obtained from the patients of the Daping Hospital, Army Medical Center of PLA (Chongqing, China) and then stored at -80°C. This research was approved by the Ethics Review Committees of Daping Hospital, Army Medical Center of PLA. Written informed consent was provided by all participants.

The human retinal pigment epithelial cell line (ARPE-19) and two retinoblastoma cell lines (Y79 and WERI-Rb-1) were provided by the American Type Culture Collection (ATCC; Manassas, VA, USA). Two RB cell lines (SO-Rb50 and HXO-RB44) were obtained from ScienCell Research Laboratories (San Diego, CA, USA). These cells were maintained in Dulbecco's Modified Eagle's Medium (DMEM; Gibco, Rockville, MD, USA) with 10% fetal bovine serum (FBS; HyClone, South-Logan, UT, USA) and 1% penicillin/streptomycin (Millipore, Billerica, MA, USA) at 37°C with 5% CO₂.

RNA Extraction and Quantitative Real-Time Polymerase Chain Reaction (qRT-PCR)

Total RNA in RB tissues/cells was obtained using TRIzol reagents (Invitrogen, Carlsbad, CA, USA). Then, SuperScript III[®] (Invitrogen, Carlsbad, CA, USA) was employed to generate complementary DNA (cDNA). Subsequently, qRT-PCR was carried out using an SYBR Premix ExTaq kit (TaKaRa Bio, Otsu, Shiga, Japan). The data were normalized to U6 level or glyceraldehyde 3-phosphate dehydrogenase (GAPDH) level with the use of the 2^{-ΔΔCt} method. The primers used in this research were:

Circ_0000034 (forward (F), 5'-GAAGCATGGGTGTGTATCC-3'; Reverse (R), 5'-GGC-CATCTCTCTCACAGCAT-3'), miR-361-3p (F, 5'-UCCCCCAGGUGUGAUUCUGAUUU-3'; R, 5'-GCAAATCAGAATCACACCTG-3'), STX17 (F, 5'-TCGTGGGAAACCTTAGAAGCGG-3'; R, 5'-GCAGCACTGTTGACATGGTCTG-3'), U6 (F, 5'-TGCGGGTGCTCGCTTCGGCAGC-3'; R, 5'-CCAGTGCAGGGTCCGAGGT-3'), and glyceraldehyde 3-phosphate dehydrogenase (GAPDH) (F, 5'-ATCACTGCCACCCAGAAGAC-3'; R, 5'-TTTCTAGACGGCAGGTCAGG-3').

RNase R Treatment

3 U/μg of RNase R (Epicentre Biotechnologies, Madison, WI, USA) was applied to treat total RNA (5 μg) for 15 min twice at 37°C.

Cell Transfection

Small interfering RNA against circ_0000034 and STX17 (si-circ_0000034#1, si-circ_0000034#2, si-circ_0000034#3, and si-STX17), small hairpin RNA against circ_0000034 (sh-circ_0000034), miR-361-3p mimic (miR-361-3p), miR-361-3p inhibitor (anti-miR-361-3p), and negative controls (si-NC, sh-NC, miR-NC, and anti-miR-NC) were provided by GenePharma (Shanghai, China). Circ_0000034 sequence was cloned into the pcDNA3.1 vector (GenePharma, Shanghai, China) to construct circ_0000034 overexpression vector. Cell transfection was performed using Lipofectamine 3000 (Invitrogen, Carlsbad, CA, USA).

Cell Proliferation Assay

The 3-(4, 5-dimethylthiazol-2-yl)-2, 5-diphenyltetrazolium bromide (MTT) kit (Promega, Madison, WI, USA) was employed to examine cell proliferation based on the user's manual. Briefly, transfected Y79 or WERI-Rb-1 cells were cultured for 24 h, 48 h, or 72 h, respectively. Then, the cells were collected, treated with MTT solution, and incubated by dimethyl sulfoxide (DMSO). Finally, the absorbance was analyzed using a microplate reader (Bio-Rad, Hercules, CA, USA) at 570 nm.

Cell Apoptosis Assay

Cell apoptosis was investigated using the Annexin V-fluorescein isothiocyanate (FITC)/propidium iodide (PI) Kit (Vazyme Biotech, Nanjing, China) in line with the recommended protocol. Briefly, transfected Y79 or WERI-Rb-1 cells were harvested, washed, and stained using Annexin V-FITC and PI. Subsequently, the flow

cytometry (BD Biosciences, San Jose, CA, USA) was applied to analyze the apoptosis rate.

Cell Migration and Invasion Assay

Transfected Y79 or WERI-Rb-1 cells in 100 μ L medium without FBS were introduced into the top transwell chamber (BD Biosciences, San Jose, CA, USA). 500 μ L medium with 10% FBS was added into the bottom chamber. After 24 h of incubation, the cells on top chamber were wiped off, and migratory cells were counted using a microscope. The matrigel (BD Biosciences, Franklin Lakes, NJ, USA) was coated on the insert of the chamber for invasion assay, and the steps were consistent with that in the migration assay.

Western Blot Assay

Total proteins in RB tissues or cells were isolated using lysis buffer (Beyotime Biotechnology, Shanghai, China). Then, Western blot assay was carried out as described previously²¹. The primary antibodies against B-cell lymphoma 2 (Bcl-2), cleaved caspase3 (C-caspase3), Cyclin D1, matrix metalloproteinase-9 (MMP-9), sequestosome 1 (P62), microtubule-associated protein 1 light chain 3 alpha (LC3-I), LC3-II, Beclin-1, STX17, and GAPDH were obtained from Abcam (Cambridge, MA, USA). Corresponding secondary antibodies were also provided by Abcam.

Mouse Xenograft

5-week-old female SCID mice were used. This experiment was approved by the Animal Research Committee of Daping Hospital, Army Medical Center of PLA and performed based on the guidance of the National Animal Care and Ethics Institution. In brief, Y79 cells transfected with sh-circ_0000034 or sh-NC were subcutaneously injected into the mice. Then, tumor volume ($\text{length} \times \text{width}^2/2$) was analyzed every 4 d. After 28 d, tumors were taken out, and tumor weight was calculated.

The Dual-Luciferase Reporter Assay

The pGL3 vector (Promega, Madison, WI, USA) inserted with wild circ_0000034 or STX17 3'UTR (wt-circ_0000034 or wt-STX17 3'UTR) or mutated circ_0000034 or STX17 3'UTR (mut-circ_0000034 or mut-STX17 3'UTR) at binding sites of miR-361-3p was co-transfected into Y79 and WERI-Rb-1 cells with miR-361-3p or miR-NC. Subsequently, the

dual-luciferase system (Promega, Madison, WI, USA) was employed to detect the Luciferase density.

RNA Immunoprecipitation (RIP) Assay

RIP assay was conducted using the Magna RNA immunoprecipitation kit (Millipore, Billerica, WI, USA) based on the recommended instruction. Briefly, Y79 or WERI-Rb-1 cells were lysed by RIP buffer, and next incubated by magnetic beads coated with anti-Argonaute2 (AGO2) or anti-Immunoglobulin G (IgG) antibodies. Finally, qRT-PCR assay was employed to investigate the RNA enrichment.

Statistical Analysis

Statistical analysis was carried out using the Student's-*t* test. The data, from three independent experiments, were shown as means \pm standard deviation (SD). The analysis of Spearman correlation was employed to investigate the relationship between the levels of two genes. When $p < 0.05$ the difference was considered significant.

Results

Circ_0000034 Expression Was Upregulated in RB Tissues and Cells

Firstly, we performed qRT-PCR assay to detect the level of circ_0000034 in RB tissues. The results suggested that circ_0000034 level was higher in RB tissues than that in normal tissues (Figure 1A). Also, circ_0000034 expression was significantly upregulated in RB cells (Figure 1B). Next, the association between circ_0000034 expression and overall survival rate of RB patients was investigated. As shown in Figure 1C, the survival rate of RB patients with a low circ_0000034 level was higher than the survival rate of RB patients with a high circ_0000034 level. The clinical characteristics of patients and the expression of circ_0000034 was demonstrated in Table I. Besides, we analyzed whether circ_0000034 exerts function as a stable circRNA by using RNase R that degraded linear RNA characterized by free 3' terminal end. The results demonstrated that RNase R did not affect circ_0000034, whereas the internal control DHDD5 was degraded (Figure 1D and E). These data indicated that circ_0000034 might act as an oncogene in RB development.

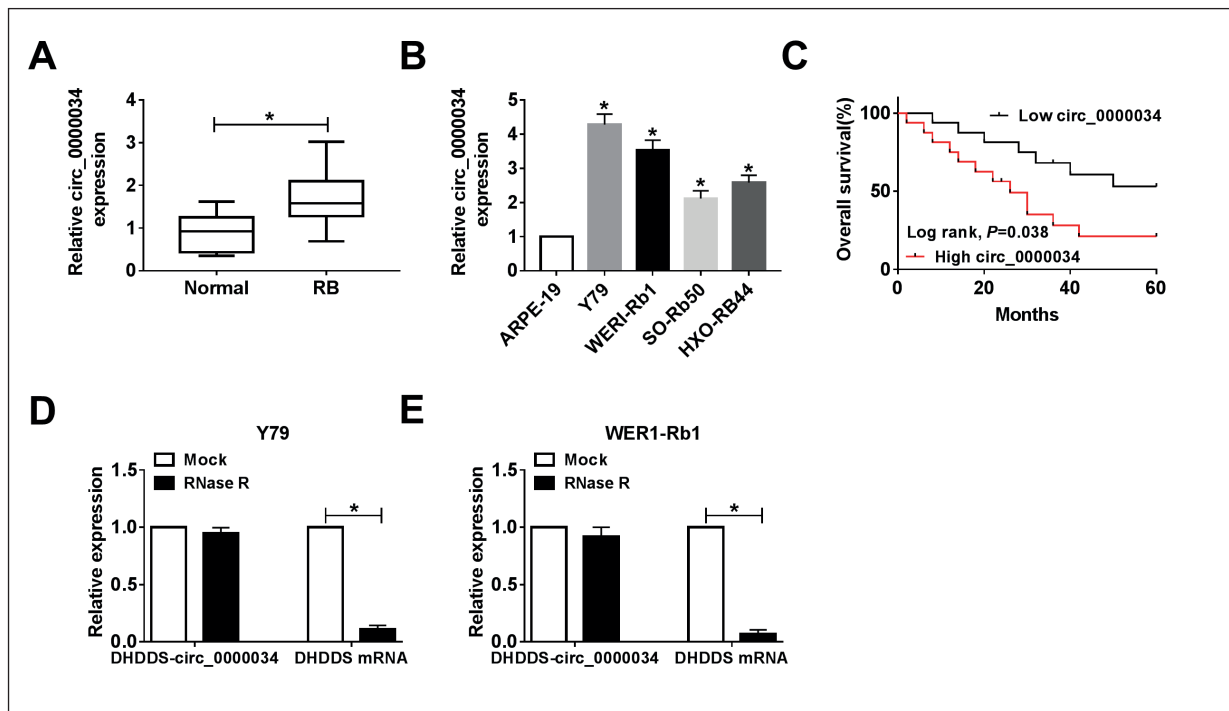


Figure 1. The level of circ_0000034 in RB tissues and cells. **A**, and **B**, Circ_0000034 level was detected by qRT-PCR assay in RB and normal tissues (**A**) as well as in RB and normal cells (**B**). **C**, Circ_0000034 level was determined in RB patients with different survival rate. **D**, and **E**, The levels of circ_0000034 and DHDDS were measured after the treatment of RNase R. * $p < 0.05$.

Table I. Clinicopathological factors and circ_0000034 expression in patients with retinoblastoma.

Parameter	Case	circ_0000034 expression		p-value ^a
		High (n=16)	Low (n=16)	
Gender				
Female	13	7	6	0.703
Male	19	9	10	
Age (years)				
≤ 60	17	10	7	0.212
> 60	15	6	9	
Choroidal invasion				
No	19	7	12	0.013*
Yes	13	9	4	
Optic nerve invasion				
No	18	6	12	0.008*
Yes	14	10	4	
Laterality				
Unilateral	23	10	13	0.124
Bilateral	9	6	3	
Pathologic grade				
Well differentiated	11	5	6	0.728
Poorly differentiated	21	11	10	

Circ_0000034 Knockdown Suppressed Cell Proliferation, Migration, Invasion, and Autophagy, and Induced Apoptosis of RB Cells

To further analyze the function of circ_0000034 in RB cells, Y79 and WERI-Rb-1 cells were transfected with si-NC, si-circ_0000034#1, si-circ_0000034#2, or si-circ_0000034#3 to knockdown the level of circ_0000034. Knockdown efficiency was confirmed by qRT-PCR assay (Figure 2A). Then, MTT assay was applied to assess cell proliferation. As demonstrated in Figure 2B and C, cell proliferation was significantly suppressed by circ_0000034 knockdown. Moreover, flow cytometry analysis showed that circ_0000034 knockdown dramatically induced cell apoptosis (Figure 2D). Also, we analyzed cell mobility, and found that cell migratory and invasive abilities were remarkably repressed by circ_0000034 knockdown in Y79 and WERI-Rb-1 cells (Figure 2E and F). Besides, the levels of some proteins, including apoptosis-related proteins (Bcl-2 and C-caspase3), proliferation-related protein (cyclin D1), invasive-related protein (MMP-9), and autophagy-related proteins (P62, LC3-I, LC3-II, Beclin-1), were detected by Western blot assay. The results demonstrated that the levels of Bcl-2, cyclin D1, MMP-9, LC3-II/LC3-I, and Beclin-1 were downregulated, and the levels of C-caspase3 and P62 were upregulated in circ_0000034-depleted Y79 and WERI-Rb-1 cells (Figure 2G-H). These data indicated that circ_0000034 depletion inhibited the growth of RB cells.

Circ_0000034 Knockdown Repressed Tumor Growth In Vivo

Next, the effect of circ_0000034 on tumor growth was explored *in vivo*. Firstly, the mice were injected with Y79 transfected with sh-NC or sh-circ_0000034. Then, tumor volume was analyzed every 4 d. As shown in Figure 3A, tumor volume was smaller in sh-circ_0000034 group compared with that in sh-NC group. After 28 d, the mice were killed, and the tumor weight was measured. The results suggested that circ_0000034 knockdown significantly downregulated tumor weight (Figure 3B). Furthermore, we determined the level of circ_0000034. As expected, circ_0000034 level was decreased in sh-circ_0000034 group (Figure 3C). Therefore, circ_0000034 depletion suppressed tumor growth *in vivo*.

MiR-361-3p Was a Target of Circ_0000034

Bioinformatics analysis tool starBase suggested that circ_0000034 possessed a complementary sequence with miR-361-3p, meaning that circ_0000034 likely interacted with miR-361-3p (Figure 4A). Then, the Dual-Luciferase reporter assay was performed to verify this interaction. As shown in Figure 4B and C, miR-361-3p overexpression reduced the Luciferase of wt-circ_0000034 but did not affect the luciferase activity of mut-circ_0000034, revealing that circ_0000034 targeted miR-361-3p. Moreover, the interaction between circ_0000034 and miR-361-3p was confirmed by RIP assay (Figure 4D and E). Subsequently, we analyzed the level of miR-361-3p in RB tissues and found that miR-361-3p level was downregulated (Figure 4F). In addition, miR-361-3p level was negatively correlated with circ_0000034 level in RB tissues (Figure 4G). Similarly, decreased miR-361-3p expression was observed in RB cells compared with normal cells (Figure 4H). On the other hand, whether circ_0000034 regulating miR-361-3p expression was explored through transfecting circ_0000034 or si-circ_0000034 into Y79 and WERI-Rb-1 cells. QRT-PCR assay firstly confirmed that the transfection with circ_0000034 increased its level (Figure 4I), and then suggested that miR-361-3p level was upregulated by circ_0000034 knockdown and downregulated by circ_0000034 overexpression (Figure 4J and K). These data revealed that circ_0000034 targeted miR-361-3p and downregulated miR-361-3p expression.

Circ_0000034 overexpression weakened the effect of miR-361-3p upregulation on RB cells

To investigate whether circ_0000034 mediating RB cell growth through inhibition of miR-361-3p expression, Y79 and WERI-Rb-1 cells were transfected with miR-NC, miR-361-3p, miR-361-3p + Vector, or miR-361-3p + circ_0000034, respectively. QRT-PCR assay verified that miR-361-3p expression was upregulated by the transfection with miR-361-3p, and then downregulated by circ_0000034 overexpression (Figure 5A). Subsequently, cell proliferation ability was investigated using MTT assay. As shown in Figure 5B and C, miR-361-3p upregulation suppressed cell proliferation, whereas this action was impaired by circ_0000034 overexpression. Furthermore, flow cytometry analysis revealed that the miR-361-3p upregulation-induced cell apoptosis was repressed by circ_0000034 overexpression (Figure 5D).

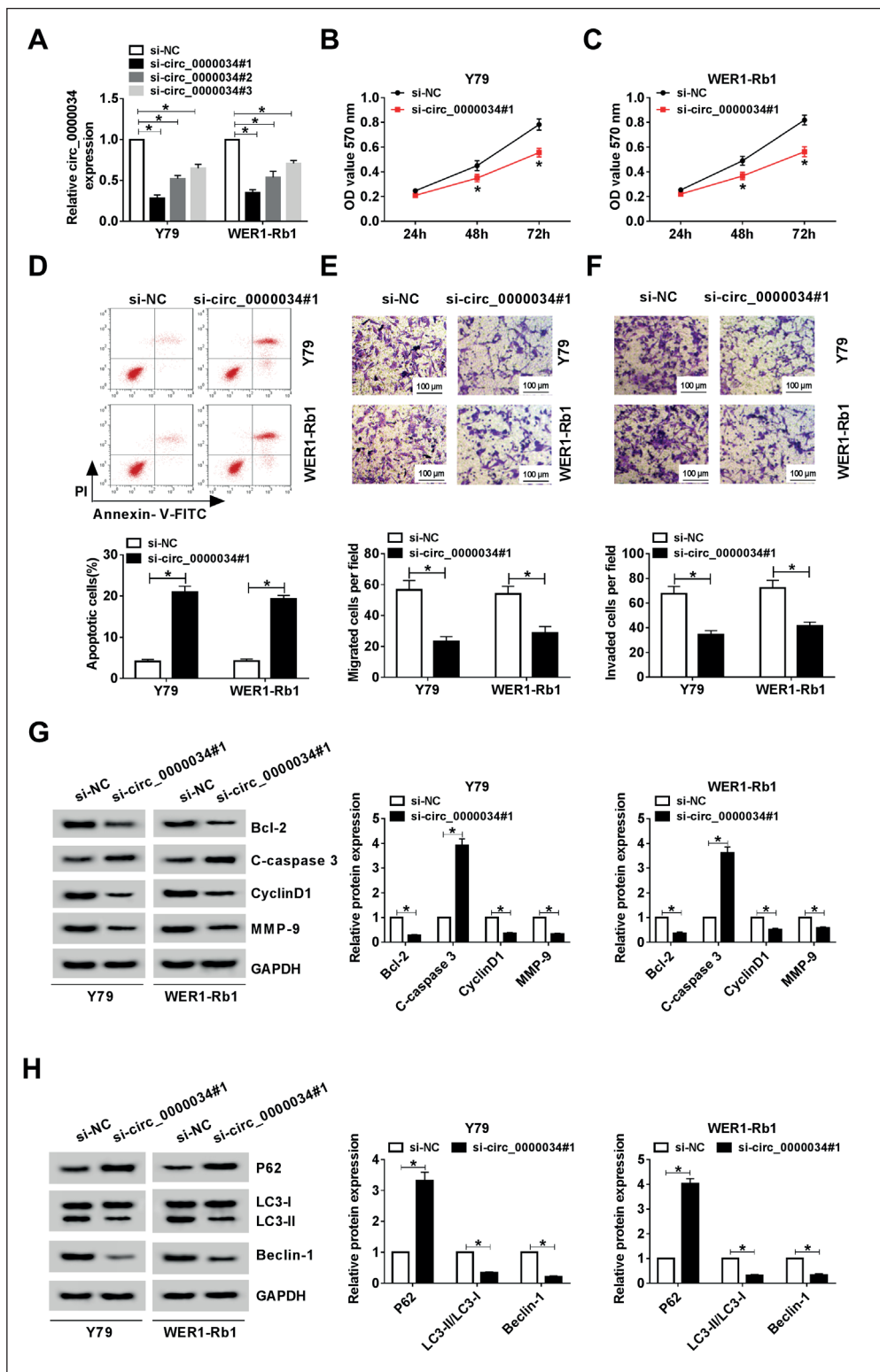


Figure 2. The function of circ_0000034 in RB cell progression. **A**, Circ_0000034 expression was examined in Y79 and WER1-Rb-1 cells transfected with si-NC, si-circ_0000034#1, si-circ_0000034#2, or si-circ_0000034#3, respectively. **B**, and **C**, MTT assay was performed to determine cell proliferation ability. **D**, Flow cytometry was used to analyze cell apoptosis rate. **E**, and **F**, Cell migratory and invasive abilities were assessed by transwell assay (100 \times). **G**, and **H**, The levels of the proteins related to proliferation, apoptosis, migration, and autophagy were detected by Western blot assay. * p <0.05.

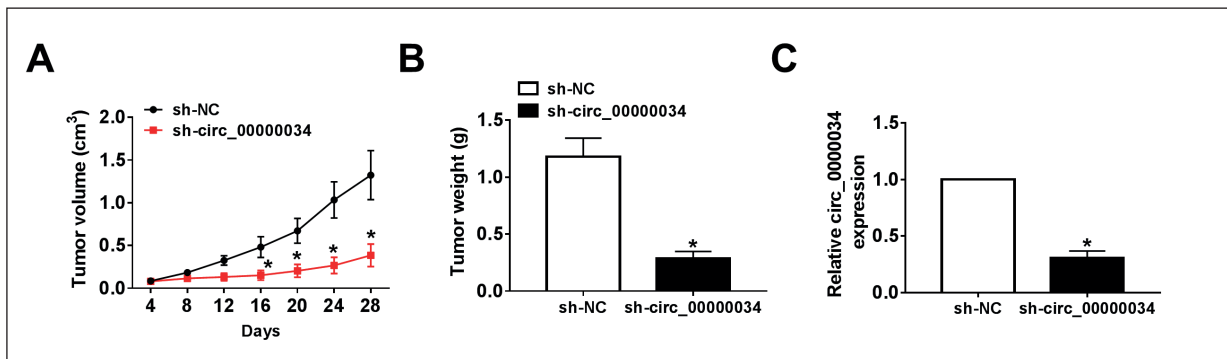


Figure 3. The effect of circ_0000034 depletion on tumor growth in vivo. **A**, and **B**, Tumor volume (**A**) and weight (**B**) were analyzed in sh-circ_0000034 group and sh-NC group. **C**, Circ_0000034 level was detected. * $p < 0.05$.

Besides, cell migratory and invasive abilities were inhibited by miR-361-3p upregulation, and then partly rescued due to circ_0000034 overexpression (Figure 5E and F). On the other hand,

we determined the levels of Bcl-2, C-caspase3, cyclin D1, MMP-9, P62, LC3-I, LC3-II, and Beclin-1, and found that circ_0000034 overexpression weakened the effect of miR-361-3p upregula-

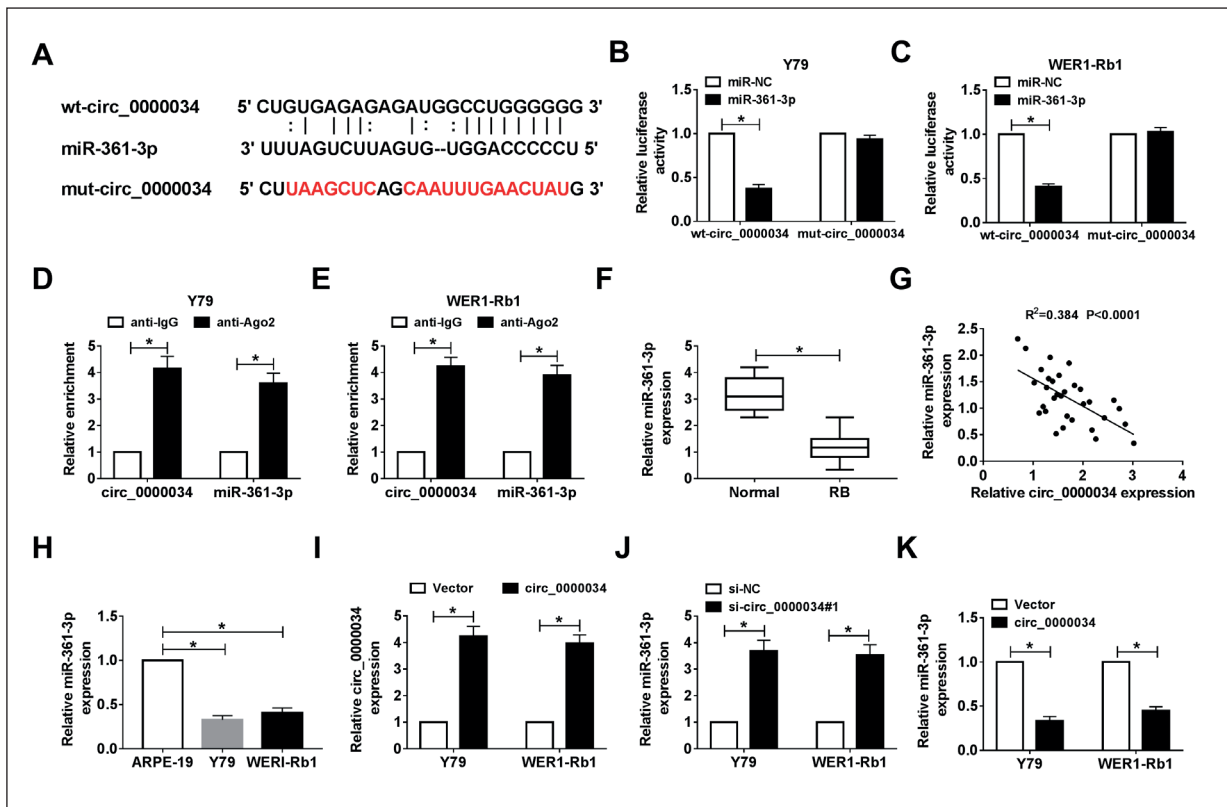


Figure 4. The relationship between circ_0000034 and miR-361-3p. **A**, The interaction between circ_0000034 and miR-361-3p was predicted by starBase. Mutated sites were expressed as the red color. **B**, and **C**, The Luciferase activity of Y79 and WER1-Rb-1 cells transfected with wt-circ_0000034 or mut-circ_0000034 and miR-361-3p or miR-NC was determined. **D**, and **E**, RIP was carried out to verify the interaction between circ_0000034 and miR-361-3p. **F**, MiR-361-3p expression was detected in RB and normal tissues. **G**, The relationship between circ_0000034 level and miR-361-3p level was analyzed. **H**, MiR-361-3p expression was measured in RB and normal cells. **I**, Circ_0000034 level was examined in Y79 and WER1-Rb-1 cells transfected with Vector or circ_0000034. **J**, and **K**, MiR-361-3p level was investigated in Y79 and WER1-Rb-1 cells transfected with si-circ_0000034 or circ_0000034. * $p < 0.05$.

tion on the levels of these proteins (Figure 5G-J). These results suggested that circ_0000034 down-regulated miR-361-3p expression to modulate RB cell progression.

MiR-361-3p Was a Sponge for STX17

Bioinformatics analysis tool starBase predicted that STX17 was a potential target gene of miR-361-3p (Figure 6A). To verify this pre-

diction, the Dual-Luciferase reporter assay was carried out. As demonstrated in Figure 6B and C, the Luciferase activity of wt-STX17 3'UTR, but not mut-STX17 3'UTR, was decreased by miR-361-3p overexpression, confirming the interaction between miR-361-3p and STX17. Then, the expression of STX17 in RB tissues was determined by qRT-PCR assay and Western blot assay. The results demonstrated that STX17 ex-

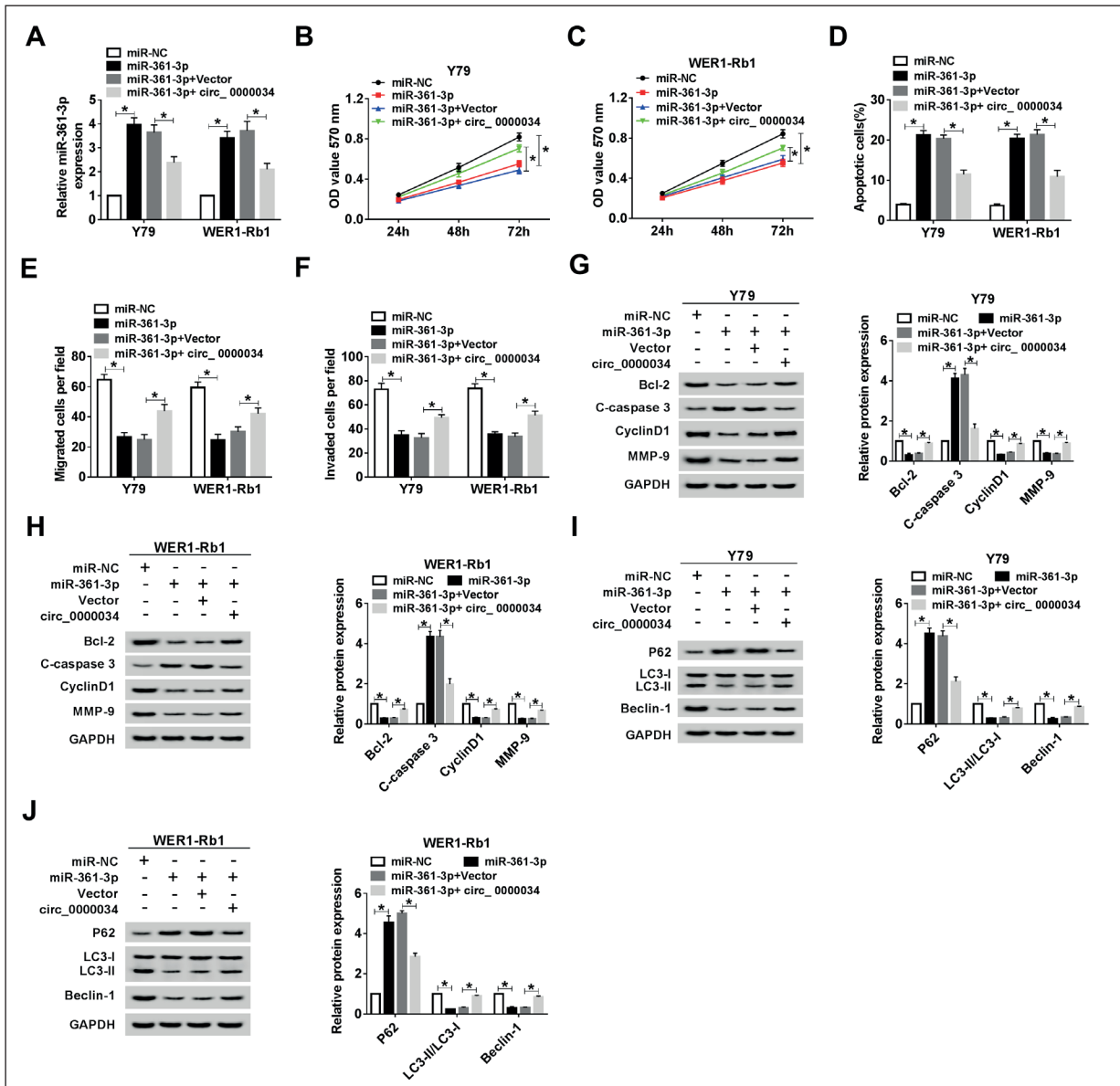


Figure 5. The effect of circ_0000034 on miR-361-3p-regulated RB cell progression. **A**, MiR-361-3p expression was detected in Y79 and WER1-Rb-1 cells transfected with miR-NC, miR-361-3p, miR-361-3p + Vector, or miR-361-3p + circ_0000034, respectively. **B**, and **C**, Cell proliferation ability was assessed using MTT assay. **D**, Cell apoptosis rate was explored using flow cytometry. **E**, and **F**, Transwell assay was employed to measure cell migratory and invasive abilities. **G-J**, Western blot was carried out to detect the levels of proteins. * $p < 0.05$.

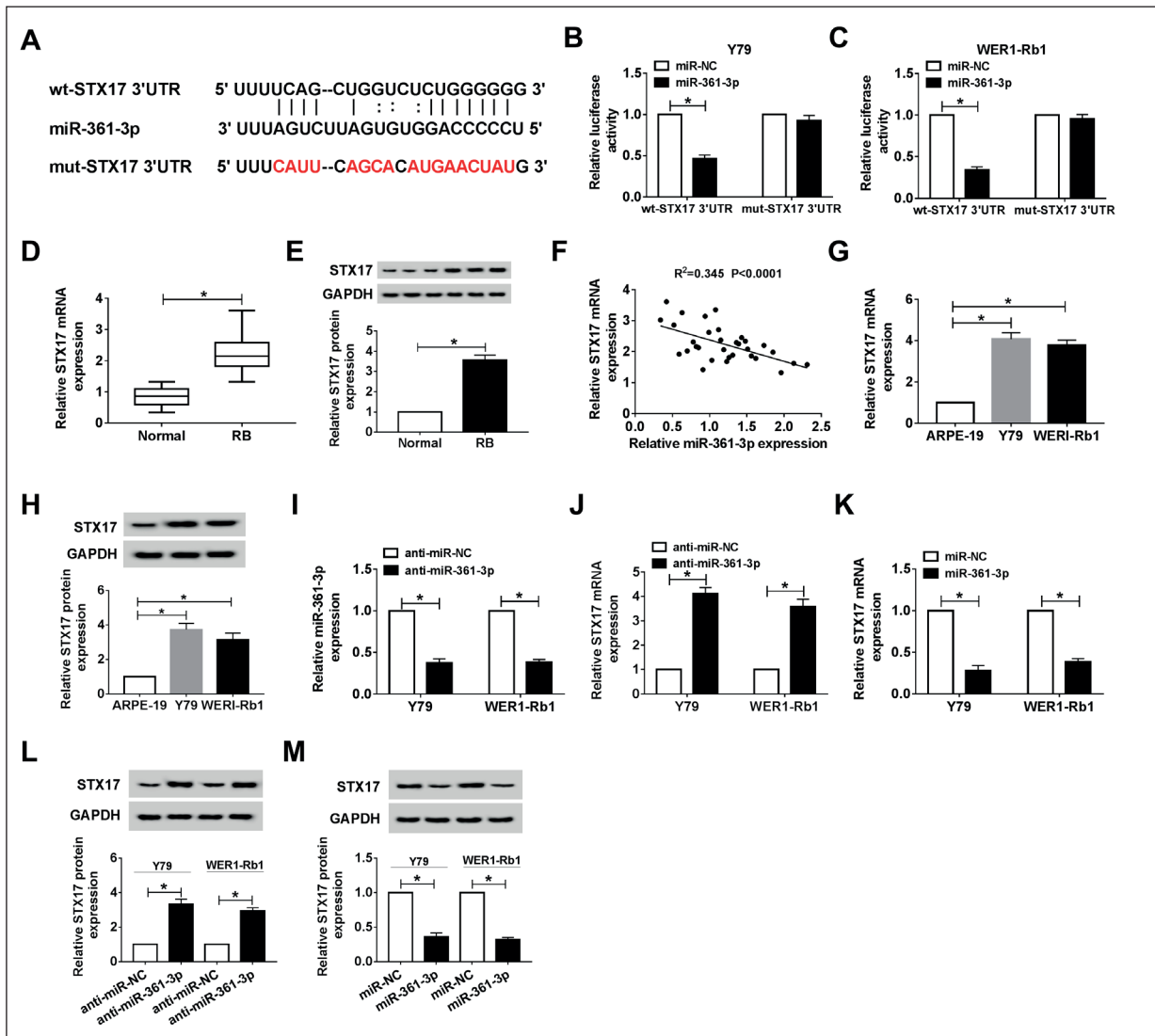


Figure 6. The relationship between miR-361-3p and STX17. **A**, StarBase was used to predict the potential targets of miR-361-3p. **B**, and **C**, The Luciferase activity was examined in Y79 and WERI-Rb-1 cells transfected with wt-STX17 3'UTR or mut-STX17 3'UTR and miR-361-3p or miR-NC. **D**, and **E**, STX17 level was detected in RB and normal tissues. **F**, The relationship between miR-361-3p level and STX17 level was investigated. **G**, and **H**, STX17 level was measured in RB and normal cells. **I**, MiR-361-3p expression was examined in Y79 and WERI-Rb-1 cells transfected with anti-miR-NC or anti-miR-361-3p. **J-M**, The mRNA level and protein level of STX17 were determined in Y79 and WERI-Rb-1 cells transfected with anti-miR-361-3p or miR-361-3p. * $p < 0.05$.

pression was higher in RB tissues than that in normal tissues (Figure 6D and E). Moreover, we analyzed the relationship between miR-361-3p level and STX17 level and found that STX17 level was negatively correlated with miR-361-3p level in RB tissues (Figure 6F). Besides, an increased STX17 level was discovered in RB cells compared with normal cells (Figure 6G and H). Next, the effect of miR-361-3p on STX17 expression was investigated through transfecting

anti-miR-361-3p or miR-361-3p into Y79 and WERI-Rb-1 cells. Firstly, we confirmed that the transfection with anti-miR-361-3p remarkably downregulated miR-361-3p expression (Figure 6I). Then, qRT-PCR assay and Western blot assay indicated that STX17 level was upregulated by miR-361-3p depletion and downregulated by miR-361-3p overexpression (Figure 6J-M). Thus, miR-361-3p repressed STX17 expression via interaction.

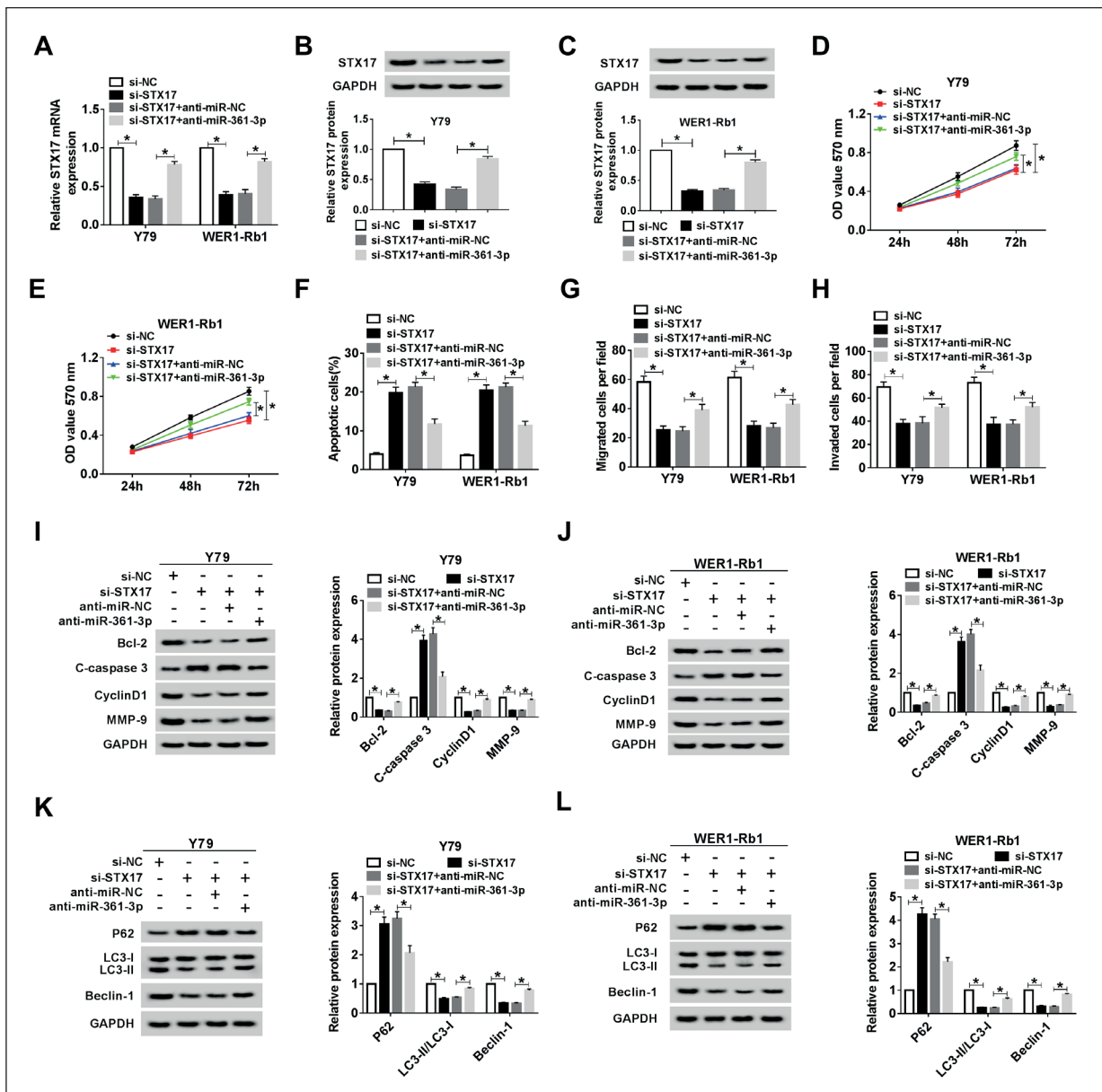


Figure 7. The effect of miR-361-3p on STX17-regulated RB cell progression. **A-C**, The mRNA level and protein level of STX17 were measured in Y79 and WER1-Rb-1 cells transfected with si-NC, si-STX17, si-STX17 + anti-miR-NC, or si-STX17 + anti-miR-361-3p, respectively. **D**, and **E**, MTT assay was conducted to analyze cell proliferation ability. **F**, Flow cytometry was used to investigate cell apoptosis rate. (**G** and **H**) Transwell assay was performed to explore cell migratory and invasive abilities. **I-L**, Western blot assay was carried out to detect the levels of proteins. $*p < 0.05$.

MiR-361-3p Depletion Reversed the Effect of STX17 Knockdown on RB Cells

To investigate whether miR-361-3p exerts function by regulating STX17 expression, Y79 and WER1-Rb-1 cells were transfected with si-NC, si-STX17, si-STX17 + anti-miR-NC, or si-STX17 + anti-miR-361-3p, respectively. QRT-PCR assay and Western blot assay confirmed that the

expression of STX17 was downregulated by the transfection with si-STX17, and then, upregulated by miR-361-3p depletion (Figure 7A-C). Subsequently, MTT assay was employed to determine cell proliferation ability. The results suggested that cell proliferation was suppressed by STX17 knockdown, and then, partly rescued due to miR-361-3p depletion (Figure 7D and E). Furthermore, flow cytometry analysis revealed that STX17

knockdown-induced cell apoptosis was inhibited by miR-361-3p depletion in Y79 and WERI-Rb-1 cells (Figure 7F). Besides, we detected cell mobility using transwell assay. As shown in Figure 7G and H, the inhibitory effect of STX17 knockdown on cell migration and invasion was impaired by miR-361-3p depletion. On the other hand, we analyzed the levels of Bcl-2, C-caspase3, cyclin D1, MMP-9, P62, LC3-I, LC3-II, and Beclin-1, and found that miR-361-3p depletion weakened the effect of STX17 knockdown on the levels of these proteins (Figure 7I-L). Taken together, miR-361-3p downregulated STX17 expression to modulate the growth of RB cells.

Circ_0000034 Inhibited MiR-361-3p Expression to Upregulate STX17 Level

In this study, we analyzed the relationship between STX17 and circ_0000034 and found that there was a positive correlation between STX17 level and circ_0000034 level in RB tissues (Figure 8A). Then, we demonstrated that the level of STX17 was downregulated by circ_0000034 knockdown, and then, partly rescued by miR-361-3p depletion (Figure 8B-D). Therefore, circ_0000034 increased the level of STX17 by repressing miR-361-3p expression.

Discussion

In recent years, more and more circRNAs were reported to be involved in the development of human cancers. So far, Li et al²² revealed that circ_0137606 inhibited the growth and metastasis of bladder cancer cells through targeting miR-1231. Ma et al²³ observed that circ_0005576 repressed cell development *via* modulating miR-153/kinesin family member 20A (KIF20A) axis in cervical cancer. Ye et al²⁴ demonstrated that circFBXW7 attenuated cell proliferation and mobility, as well as tumor growth, by mediating miR-197-3p level in breast cancer. Therefore, circRNAs exerted a crucial function in human cancers. However, the researches of circRNAs in RB were little. In this study, we found that circ_0000034 expression was significantly increased in RB tissues and cells. This result was consistent with the previous data¹⁰. Furthermore, we observed that circ_0000034 knockdown inhibited RB cell proliferation, mobility, and autophagy, as well as induced apoptosis. These results suggested that circ_0000034 acted as an oncogene in RB development. Nowadays, the study of circ_0000034 function in human cancers is rare. Therefore, more experiments are needed to verify

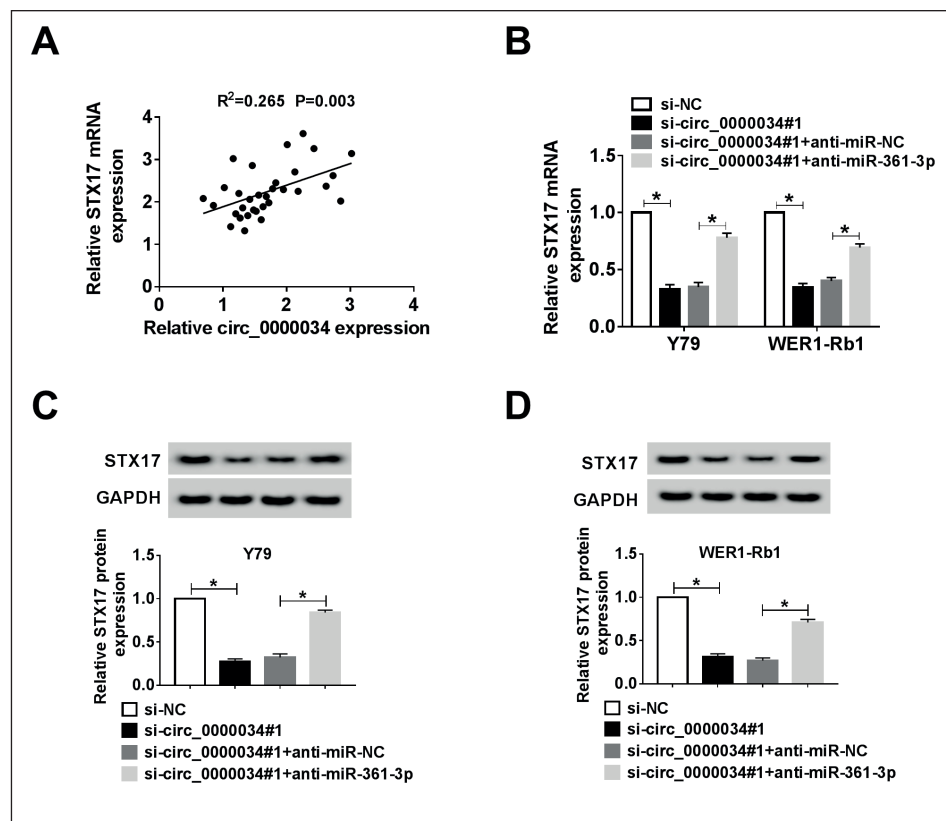


Figure 8. The association among circ_0000034, miR-361-3p, and STX17. **A**, The relationship between circ_0000034 level and STX17 level was analyzed. **B-D**, The expression of STX17 was determined in Y79 and WERI-Rb-1 cells transfected with si-NC, si-circ_0000034#1, si-circ_0000034#1 + anti-miR-NC, or circ_0000034#1 + anti-miR-361-3p, respectively. **p*<0.05.

the function of circ_0000034 in human cancers.

CircRNA mediated the development of cancer cells through targeting miRNAs and downregulating the level of target miRNA in human cancers^{25,26}. For instance, circRNA UBAP2 reduced miR-144 level via sponging miR-144 in ovarian cancer cells²⁷. We then used bioinformatics analysis tool starBase to explore the downstream genes of circ_0000034 and found that miR-361-3p was a potential target of circ_0000034. Subsequently, the interaction between circ_0000034 and miR-361-3p was proved by the Dual-Luciferase reporter assay and RIP assay. Moreover, we revealed that circ_0000034 downregulated the level of miR-361-3p. MiR-361-3p, considered as a tumor suppressor, was shown to repress the development of many cancers. In particular, miR-361-3p attenuated the growth of non-small cell lung cancer cells by modulating the level of SH2B adaptor protein 1 (SH2B1)²⁸. Liu et al²⁹ revealed that miR-361-3p level was significantly low in cervical cancer tissues. Here, we analyzed the expression and function of miR-361-3p in RB. The results indicated that miR-361-3p level was decreased in RB tissues and cells, as well as miR-361-3p suppressed the growth of RB cells. These results were accordant with the previous data¹⁷. Taken together, we speculated that circ_0000034 inhibited miR-361-3p expression to modulate RB cell progression. Further, this hypothesis was confirmed by our experiments.

Present evidence^{30,31} demonstrated that miRNA acted as a sponge for mRNA via binding the 3'UTR of mRNA in human cancers. To further investigate the functional mechanism of miR-361-3p, bioinformatics analysis tool starBase was used to predict the potential targets of miR-361-3p. The results showed that STX17 likely interacted with miR-361-3p. Then, the interaction between STX17 and miR-361-3p was verified by the Dual-Luciferase reporter assay. Furthermore, our results confirmed that STX17 level was downregulated by miR-361-3p. STX17 was initially reported as a cell autophagy-related protein. STX17 interacted with the target protein to promote the information of the autophagosome^{18,32}. Moreover, Hamasaki et al³³ indicated that the depletion of STX17 impaired the function of the autophagosome. Thereafter, it has been shown that STX17 level was increased in RB cells, and STX17 accelerated RB cell autophagy²⁰. In this study, we analyzed the expression and function of STX17 in RB cells. The results were in agreement with the previous data. Furthermore, we also detected

that STX17 knockdown inhibited cell proliferation and mobility and promoted apoptosis in RB. Besides, STX17 knockdown repressed the growth of RB cells, whereas this effect was weakened by the depletion of miR-361-3p. Therefore, miR-361-3p suppressed the expression of STX17 to affect RB cell progression.

Conclusions

Taken together, these results showed that circ_0000034 upregulated STX17 level through inhibiting miR-361-3p expression. Our findings demonstrated that circ_0000034 knockdown inhibited the growth of RB cells via modulating miR-361-3p/STX17 axis, providing a potential target for the therapy of RB patients.

Conflict of Interests

The authors declare that they have no financial conflicts of interest.

References

- 1) BROADDUS E, TOPHAM A, Singh AD. Incidence of retinoblastoma in the USA: 1975-2004. *Br J Ophthalmol* 2009; 93: 21-23.
- 2) SHIELDS CL, SHIELDS JA. Diagnosis and management of retinoblastoma. *Cancer Control* 2004; 11: 317-327.
- 3) LIU Q, WANG Y, WANG H, LIU Y, LIU T, KUNDA PE. Tandem therapy for retinoblastoma: immunotherapy and chemotherapy enhance cytotoxicity on retinoblastoma by increasing apoptosis. *J Cancer Res Clin Oncol* 2013; 139: 1357-1372.
- 4) MEMCZAK S, JENS M, ELEFSINIOTI A, TORTI F, KRUEGER J, RYBAK A, MAIER L, MACKOWIAK SD, GREGENSEN LH, MUNSCHAUER M, LOEWER A, ZIEBOLD U, LANDTHALER M, KOCKS C, LE NOBLE F, RAJEWSKY N. Circular RNAs are a large class of animal RNAs with regulatory potency. *Nature* 2013; 495: 333-338.
- 5) JECK WR, SHARPLESS NE. Detecting and characterizing circular RNAs. *Nat Biotechnol* 2014; 32: 453-461.
- 6) CHEN G, SHI Y, ZHANG Y, SUN J. CircRNA_100782 regulates pancreatic carcinoma proliferation through the IL6-STAT3 pathway. *Onco Targets Ther* 2017; 10: 5783-5794.
- 7) ZHOU LH, YANG YC, ZHANG RY, WANG P, PANG MH, LIANG LQ. CircRNA_0023642 promotes migration and invasion of gastric cancer cells by regulating EMT. *Eur Rev Med Pharmacol Sci* 2018; 22: 2297-2303.
- 8) LV X, WANG M, QIANG J, GUO S. Circular RNA circ-PITX1 promotes the progression of glioblastoma by acting as a competing endogenous RNA to regulate miR-379-5p/MAP3K2 axis. *Eur J Pharmacol* 2019; 863: 172643.

- 9) MENG L, LIU S, DING P, CHANG S, SANG M. Circular RNA ciRS-7 inhibits autophagy of ESCC cells by functioning as miR-1299 sponge to target EGFR signaling. *J Cell Biochem* 2019 Sep 6. doi: 10.1002/jcb.29339. [Epub ahead of print]
- 10) LYU J, WANG Y, ZHENG Q, HUA P, ZHU X, LI J, LI J, JI X, ZHAO P. Reduction of circular RNA expression associated with human retinoblastoma. *Exp Eye Res* 2019; 184: 278-285.
- 11) LIU B, LI J, CAIRNS MJ. Identifying miRNAs, targets and functions. *Brief Bioinform* 2014; 15: 1-19.
- 12) BARTEL DP. MicroRNAs: genomics, biogenesis, mechanism, and function. *Cell* 2004; 116: 281-297.
- 13) MA L, ZHENG Y, TANG X, GAO H, LIU N, GAO Y, HAO L, LIU S, JIANG Z. miR-21-3p inhibits autophagy of bovine granulosa cells by targeting VEGFA via PI3K/AKT signaling. *Reproduction* 2019 Sep 1. pii: REP-19-0285.R2. doi: 10.1530/REP-19-0285. [Epub ahead of print]
- 14) ZHAO Y, XU Z, ZHOU J, YANG H. miR141 inhibits proliferation, migration and invasion in human hepatocellular carcinoma cells by directly down-regulating TGF β 1. *Oncol Rep* 2019; 42: 1656-1666.
- 15) HUANG J, WANG X, WEN G, REN Y. miRNA2055p functions as a tumor suppressor by negatively regulating VEGFA and PI3K/Akt/mTOR signaling in renal carcinoma cells. *Oncol Rep* 2019; 42: 1677-1688.
- 16) CHENG Y, LIU W. MicroRNA-503 serves an oncogenic role in retinoblastoma progression by directly targeting PTPN12. *Exp Ther Med* 2019; 18: 2285-2292.
- 17) ZHAO D, CUI Z. MicroRNA-361-3p regulates retinoblastoma cell proliferation and stemness by targeting hedgehog signaling. *Exp Ther Med* 2019; 17: 1154-1162.
- 18) ITAKURA E, KISHI-ITAKURA C, MIZUSHIMA N. The hairpin-type tail-anchored SNARE syntaxin 17 targets to autophagosomes for fusion with endosomes/lysosomes. *Cell* 2012; 151: 1256-1269.
- 19) UEMATSU M, NISHIMURA T, SAKAMAKI Y, YAMAMOTO H, MIZUSHIMA N. Accumulation of undegraded autophagosomes by expression of dominant-negative STX17 (syntaxin 17) mutants. *Autophagy* 2017; 13: 1452-1464.
- 20) HUANG J, YANG Y, FANG F, LIU K. MALAT1 modulates the autophagy of retinoblastoma cell through miR-124-mediated stx17 regulation. *J Cell Biochem* 2018; 119: 3853-3863.
- 21) SUN Y, ZHANG T, WANG C, JIN X, JIA C, YU S, CHEN J. MiRNA-615-5p functions as a tumor suppressor in pancreatic ductal adenocarcinoma by targeting AKT2. *PLoS One* 2015; 10: e0119783.
- 22) LI W, LI Y, SUN Z, ZHOU J, CAO Y, MA W, XIE K, YAN X. Comprehensive circular RNA profiling reveals the regulatory role of the hsa_circ_0137606/miR1231 pathway in bladder cancer progression. *Int J Mol Med* 2019; 44: 1719-1728.
- 23) MA H, TIAN T, LIU X, XIA M, CHEN C, MAI L, XIE S, YU L. Upregulated circ_0005576 facilitates cervical cancer progression via the miR-153/KIF20A axis. *Biomed Pharmacother* 2019; 118: 109311.
- 24) YE F, GAO G, ZOU Y, ZHENG S, ZHANG L, OU X, XIE X, TANG H. circFBXW7 inhibits malignant progression by sponging miR-197-3p and encoding a 185-aa protein in triple-negative breast cancer. *Mol Ther Nucleic Acids* 2019 Aug 14;18:88-98. doi: 10.1016/j.omtn.2019.07.023. [Epub ahead of print]
- 25) XIONG DD, FENG ZB, LAI ZF, QIN Y, LIU LM, FU HX, HE RQ, WU HY, DANG YW, CHEN G, LUO DZ. High throughput circRNA sequencing analysis reveals novel insights into the mechanism of nitidine chloride against hepatocellular carcinoma. *Cell Death Dis* 2019; 10: 658.
- 26) XU Z, SHEN J, HUA S, WAN D, CHEN Q, HAN Y, REN R, LIU F, DU Z, GUO X, SHI J, ZHI Q. High-throughput sequencing of circRNAs reveals novel insights into mechanisms of nigericin in pancreatic cancer. *BMC Genomics* 2019; 20: 716.
- 27) SHENG M, WEI N, YANG HY, YAN M, ZHAO QX, JING LJ. CircRNA UBAP2 promotes the progression of ovarian cancer by sponging microRNA-144. *Eur Rev Med Pharmacol Sci* 2019; 23: 7283-7294.
- 28) CHEN W, WANG J, LIU S, WANG S, CHENG Y, ZHOU W, DUAN C, ZHANG C. MicroRNA-361-3p suppresses tumor cell proliferation and metastasis by directly targeting SH2B1 in NSCLC. *J Exp Clin Cancer Res* 2016; 35: 76.
- 29) LIU S, SONG L, YAO H, ZHANG L, XU D, LI Q, LI Y. Preserved miR-361-3p Expression is an independent prognostic indicator of favorable survival in cervical cancer. *Dis Markers* 2018; 2018: 8949606.
- 30) LI M, GUO Q, CAI H, WANG H, MA Z, ZHANG X. miR-218 regulates diabetic nephropathy via targeting IKK- β and modulating NK- κ B-mediated inflammation. *J Cell Physiol* 2019 Sep 24. doi: 10.1002/jcp.29224. [Epub ahead of print]
- 31) HOU G, XU W, JIN Y, WU J, PAN Y, ZHOU F. MiRNA-217 accelerates the proliferation and migration of bladder cancer via inhibiting KMT2D. *Biochem Biophys Res Commun* 2019; 519: 747-753.
- 32) ITAKURA E, MIZUSHIMA N. Syntaxin 17: the autophagosomal SNARE. *Autophagy* 2013; 9: 917-919.
- 33) HAMASAKI M, FURUTA N, MATSUDA A, NEZU A, YAMAMOTO A, FUJITA N, OOMORI H, NODA T, HARAGUCHI T, HIRAOKA Y, AMANO A, YOSHIMORI T. Autophagosomes form at ER-mitochondria contact sites. *Nature* 2013; 495: 389-393.